

**Petrochemistry of Atalla I-type younger granite, Wadi Atalla area, Central Eastern Desert, Egypt:  
implication for petrogenesis and tectonic setting**

**Gamal A. Abdelhadi<sup>1\*</sup>, Gamal M. Kamal El Din<sup>1</sup>, Asran M. Hassan<sup>2</sup>, Taha M. Amroon<sup>1</sup>**

<sup>1</sup>Geology Department, Faculty of Science, South Valley University, Egypt

<sup>2</sup>Geology Department, Faculty of Science, Sohag University, Egypt

**Abstract**

*The basement rocks exposed in the area of wadi Atalla are characterized by the intrusion of I-type granites. Petrological and geochemical studies revealed that these granites are dominated by granite in composition. Petrographically, Atalla granite is composed mainly of plagioclase, K-feldspar, and quartz with subordinate amounts of biotite. Sericite, kaolinite, epidote, muscovite are alteration products while iron oxides, sphene, zircon, and apatite are common accessories. Geochemically, Atalla granite has calc-alkaline affinities with aluminium saturation index varies from weakly metaluminous to peraluminous. They were formed in volcanic arc setting under compressional regime where subduction-related environments are dominant. Field relation and trace element geochemistry of granites from wadi Atalla suggest their derivation from mantle source.*

*Key words: calc-alkaline; geochemistry; petrography; Wadi Atalla.*

**1 Introduction**

The crustal evolution of the Arabian Nubian Shield was summarized through four main stages (Gass 1982; Bentor 1985; Stern and Hedge 1985; Stern et al. 1988; Kröner et al. 1990; Stern 1993; Kröner 1993). The rifting followed by sea-floor spreading and the initiation of subduction resulted in formation of oceanic crust and island arcs terranes characterized the first and second stages that occurred at 950–850 Ma and 850–650 Ma respectively. The end of second stage was dominated by welding and accretion of oceanic and island arc terrains to form the Arabian-Nubian Shield. The third stage (650–580 Ma) is the post-collision batholithic stage. During this stage, large scale calc-alkaline magmatism, mainly of intermediate to felsic composition predominated. The post-orogenic stage represents the fourth stage (600–530 Ma) that was characterized by igneous activity of mainly alkaline to peralkaline granites, andesites, rhyolites, and several episodes of dike swarms representing intracratonic within-plate magmatism. Akaad and Noweir (1980) and El Gaby et al. (1988) termed the group of granitic rocks that evolved during the final stage as the younger granitoids. These granitic rocks represent a major component of the crust in the basement complex of Egypt. They form about 30% of the total surface exposure of the basement rocks. They range in composition from granodiorite to granite with I-type characteristics, but some have A-type affinities (Stern and Hedge, 1985; Abdel Rahman and Martin, 1990; Hassanen, 1997). Hussein et al. (1982) divided the Egyptian younger granites into suture related granites (G2-granite) formed in post-orogenic environment and intraplate granites (G3-granite) related to rifting processes. Hassan and Hashad (1990) suggested that the magma of the younger granites was emplaced in three possible tectonic settings: (1) subduction processes in a volcanic arc environment, (2) arc-continent collision event, and (3) within continental plates. Noweir et al. (1990) considered the Egyptian younger granites as transitional phases from calc-alkaline I-type magmatism to normal alkaline and peralkaline A-type granite. El-Sayed (1998) classified the Egyptian granites into I-type orogenic arc related and A-type anorogenic rift-related granites. A systematic study of particular granitic rock will provide detailed magmatic and geochemical processes that perform in particular area. There has been little systematic study of granitic rocks in wadi Atalla area, therefore, this paper aims to shed the light on the petrological and geochemical characteristics of the granitic rocks in wadi Atalla and deduce their petrogenesis and tectonic setting.

## 2 General Geology

Wadi Atalla area is located to the northwest of the well-known Fawakhair area in the Central Eastern Desert of Egypt. It covers an area of about 250 Km<sup>2</sup> of the basement complex in the Central Eastern Desert of Egypt between latitudes 26° 00' 00" & 26° 15' 00" N and longitudes 33° 30' 00" & 33° 40' 00" E (Fig.1). The general geology of wadi Atalla area is dominated by the Pan-African rocks. These rocks comprise serpentinites and related rocks (oldest), metavolcanics and their equivalent pyroclastics, metagabbro-diorite complex, Hammamat sediments, Atalla granites, Atalla felsites, and post-granitic dykes (youngest) (Fig.2). *El Kasses* (1974) and *El kasses and Bakhit* (1989) studied Wadi Atalla and Wadi Atalla- El Missikat areas respectively from the geological and radioactivity points of view and proposed a classification of the exposed rock units in the light of the geosynclinal theory. *Akaad et al*(1976) studied the area around Bir El kubbania and prepared a geological map of scale 1: 100,000 in which they described the lithostratigraphic units in the light of geosynclinal theory and arranged them chronologically. *El Bouseily et al.* (1985) mentioned that Gabal Atalla granite is alkali- to monzogranite in composition. Atalla I-type younger granite occupies the central part of the study area (Fig.2). They intrude the preexisting rock units such as metavolcanics, metagabbro, and serpentinites and intruded by numerous post granitic dykes where the contacts are very sharp in some localities. The studied granitic pluton is bounded from the south and north by metavolcanics where the contacts are sharp knife and there is no evidence for thermal effect. They take some metavolcanics as xenoliths within it. Generally, Atalla granite form moderate to high relief terrains characterized by reddish to pinkish and grey to dark greyish colours. They form a pear-like intrusion trending with its long axis in the NW direction and are dissected by minor wadies. They are highly dissected by sets of joints having variable orientations. Atalla granites are medium to coarse in grain size and include dark enclaves of intermediate composition. They are dissected by post granitic dykes that are generally mafic to felsic in composition and range from less than 30 cm to more than 3 meters in width and cut by some quartz veins of variable lengths and widths.

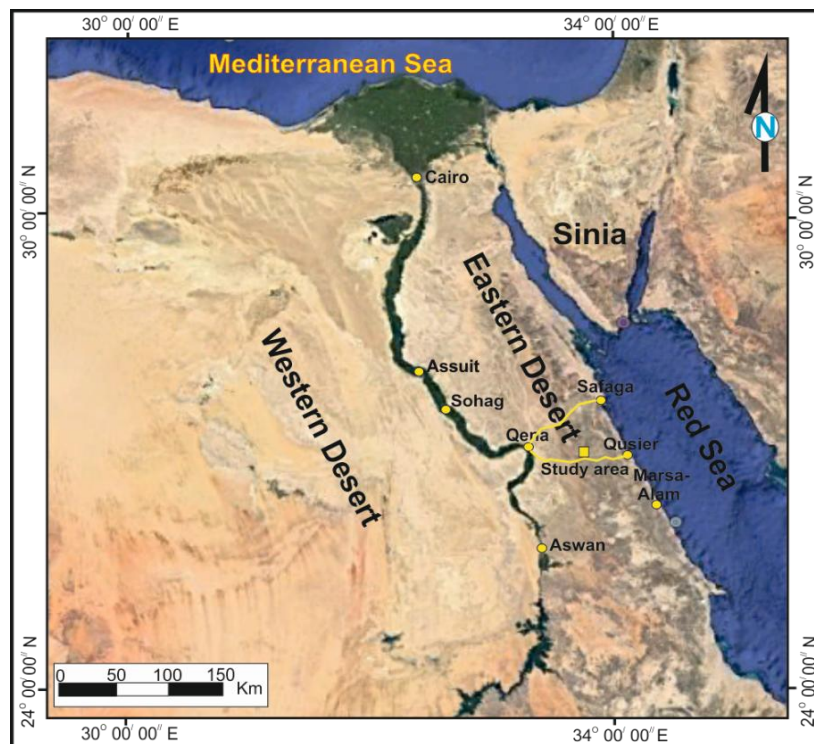


Fig.1: Location map of the study area.

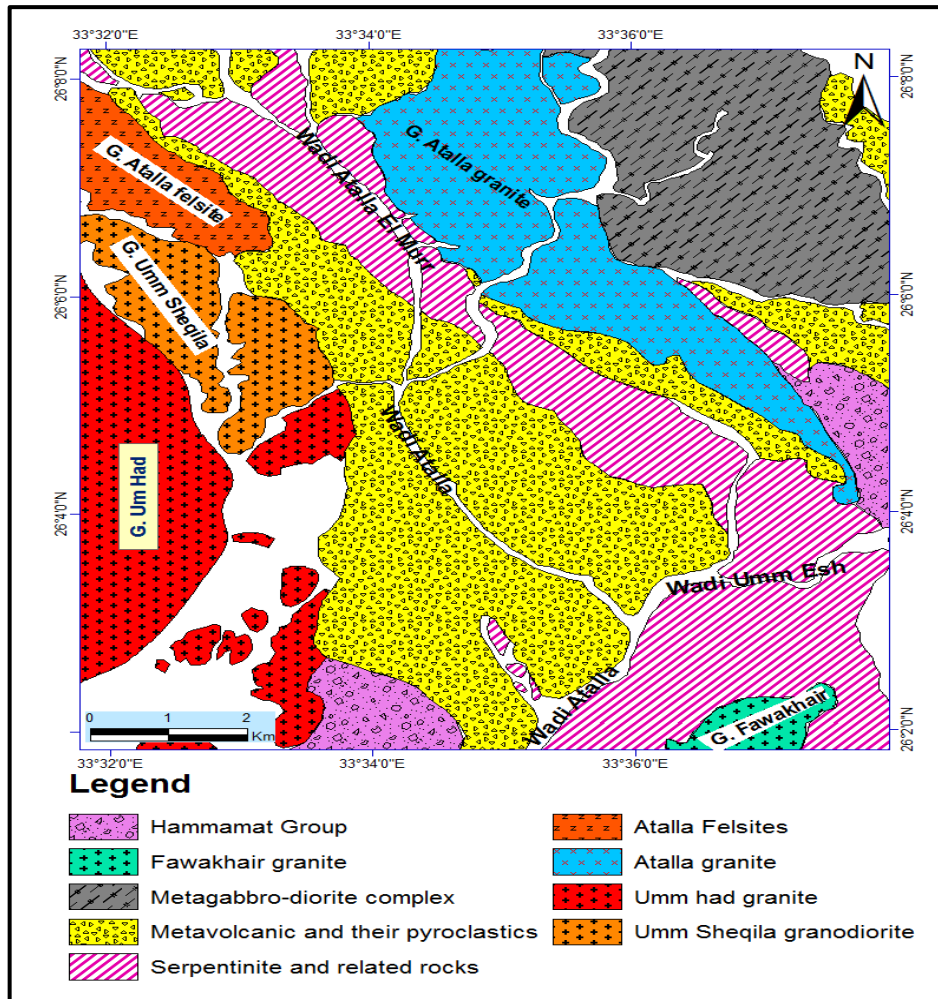


Fig.2: Geological map of wadi Atalla area

### 3 Petrography

A total of 25 thin sections of representative samples from the granitic rocks were examined. The studied granites are massive, grey and pink in colour, medium- to coarse-grained, equigranular to inequigranular, subhedral characterized by a common hypidiomorphic granular texture and contain dark enclaves of andesitic composition (Fig.3.2). The major constituent minerals are plagioclase, k-feldspar, quartz, and subordinate amounts of biotite. Zircon, apatite, and iron oxides are the common accessories. While chlorite replaced biotite and sericite and epidote are present as secondary minerals. Calcite, chlorite, epidote occur as minor constituents, muscovite, biotite are accessory minerals. **Plagioclase** occurs as euhedral to subhedral crystals of variable sizes ranging in length approximately from 1 mm to 3 mm and in width from 0.5 mm to 1.5 mm. They are moderately to highly altered to sericite and kaolinite. Muscovite, epidote, and calcite are also alteration products in the highly altered samples (Fig.3.3). Plagioclase crystals display both carlsbad-albite and polysynthetic twinning and contain inclusions of apatite and iron oxides. **K-feldspars** are represented by orthoclase perthite and microcline perthite with characteristic string and patchy perthite. In some slices, k-feldspar is replacing plagioclase crystals and consequently irregular plagioclases are enclosed within k-feldspar. Generally, feldspars occur as subhedral to anhedral tabular crystals up to 1x0.4 mm and slightly altered to sericite, kaolinite and stained by hematitic iron oxides. **Quartz** forms water clear anhedral crystals filling the irregular spaces among the other

minerals and ranging in size from 0.5 to 1.5 mm. in the slightly deformed samples, quartz displays undulatory extinction and dissected by cracks which are filled with fine grained muscovite and carbonates (Fig.3.4). It encloses iron oxide, apatite, and zircon grains and crystals as inclusions (Fig.3.5). Sometimes, quartz occurs as inclusions within plagioclase and biotite. **Biotite** occurs as small flakes and plates up to 0.4 mm long of brown colours and strongly pleochroic to yellow and dark brown and highly altered to chlorite, epidote, and iron oxides where they are aligned along the cleavage planes (Fig.3.6). Some biotite crystals are bent and displaying both undulatory extinction and kink band suggesting effect of deformation process. Few biotite crystals are perforated by quartz and dissected by microfaults. **Chlorite** occurs as alteration products of biotite where the inherited one set of cleavage plane of biotite can be traced. Chlorite forms thick patches and dense aggregates of green colour, weakly pleochroic from pale green to green colour and exhibits anomalous inky and bluish interference colour. In some samples, chlorite actively corrodes plagioclases and other constituents. **Iron oxides** occur as both accessory constituents of cubic grains and/or irregular aggregates enclosed within plagioclase, Quartz and if not, is scattered throughout the rock whereas as the secondary ones are commonly associated with biotite and chlorite. **Muscovite** occurs as alteration products of biotite and/or plagioclase. It is usually associated with chlorite when it occurs as alteration products of biotite. Muscovite displays high interference colors, and has clear one set of cleavage. **Sericite and kaolinite** occur as alteration products of fine honey aggregates after plagioclase and potash feldspar. In the highly altered samples, they mask the twinning planes of plagioclase. **Calcite** occurs either as alteration products at the expense of plagioclase indicating high stages of alterations or forms patches between the other constituents and/or as veinlets that filling the cracks. **Epidote** occurs as secondary products after biotite and plagioclase and commonly associated with chlorite. **Apatite** forms tiny euhedral tabular to acicular crystals that are commonly enclosed within plagioclases and quartz. **Zircon** occurs as tiny euhedral prismatic crystals enclosed within quartz and plagioclase. Some zircon crystals display zoning. **Clinozoisite** occurs as alteration products of plagioclase with diagnostic yellowish to abnormal bluish interference colour.

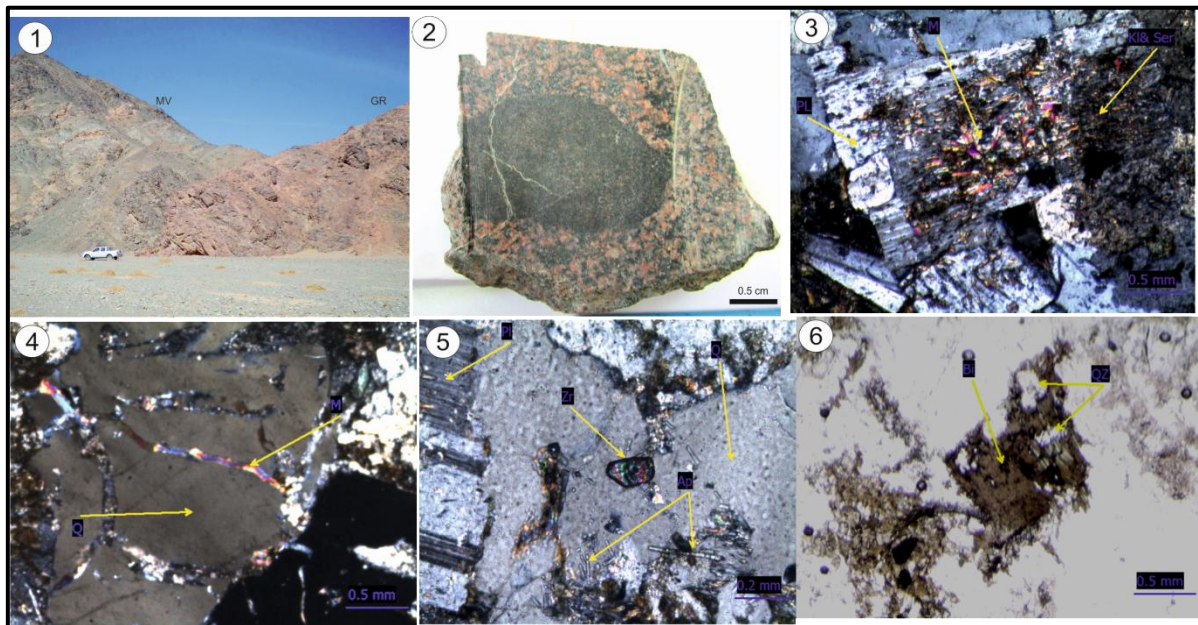


Fig.3: photograph showing 1) Sharp contact between Atalla granite and its neighbouring metavolcanics. 2) Polished slab of granitic samples includes dark enclaves of andesitic composition. 3) Highly altered plagioclase crystal. 4) Quartz crystal dissected by fractures filled by fine grained muscovite and calcite 5) Quartz crystal encloses euhedral crystal of zircon. 6) Biotite crystal perforated by quartz and is partially altered to chlorite along cleavage planes.

#### 4 Geochemistry

Eight samples were carefully selected on petrographic criteria to ensure that a complete range of compositions was obtained. Major and trace element analyses were determined by inductively coupled plasma source spectrometry techniques at ACME lab in Canada. The results of major and trace element compositions were listed in table 1.

Table 1. The result of major and trace elements composition of the studied granites

Sample	1	2	3	4	5	6	7	25
SiO <sub>2</sub>	73.27	72.19	72.35	77.76	67.11	70.04	68.03	67.61
Al <sub>2</sub> O <sub>3</sub>	13.84	14.11	13.96	11.75	15.21	14.62	14.83	14.98
Fe <sub>2</sub> O <sub>3</sub>	2.13	2.47	2.59	0.99	4.04	3.23	3.79	4.03
MgO	0.42	0.45	0.43	0.04	0.8	0.58	1.2	0.79
CaO	0.69	0.87	0.78	0.14	2.04	1.44	2.65	2.04
Na <sub>2</sub> O	4.69	4.99	4.84	3.44	5.28	4.89	4.53	4.9
K <sub>2</sub> O	3.5	3.33	3.28	5.09	2.37	3	2.72	2.97
TiO <sub>2</sub>	0.33	0.38	0.38	0.06	0.58	0.43	0.56	0.58
P <sub>2</sub> O <sub>5</sub>	0.05	0.05	0.05	0.01	0.14	0.1	0.11	0.14
MnO	0.03	0.05	0.05	<0.01	0.08	0.06	0.09	0.11
Cr <sub>2</sub> O <sub>3</sub>	<0.002	<0.002	<0.002	<0.002	<0.002	0.003	0.002	0.006
LOI	0.9	1	1.1	0.6	2.2	1.5	1.3	1.7
Sum	99.92	99.91	99.91	99.94	99.88	99.92	99.89	99.89
Trace elements (ppm)								
Ba	438	491	455	456	580	465	436	475
Sc	5	5	6	<1	8	6	8	8
Be	2	2	4	3	3	2	2	2
Co	2.2	2	1.9	1.5	4.1	3.3	6.7	3.8
Cs	0.9	0.7	0.5	0.2	1	0.5	0.8	0.2
Ga	20.3	17.9	19.5	13.9	18	18.3	17.4	17.2
Hf	9	8.2	9.1	10	9.4	8.7	7	9.3
Nb	12.4	12.2	12.9	15.3	11.2	10.2	8.3	11.5
Rb	37.7	34.6	37.8	39.2	31.5	36.3	39.5	47.5
Sn	4	3	4	2	2	2	2	2
Sr	110.3	103.5	110.7	61.8	273.5	150.4	270.5	210
Ta	1.2	0.8	0.9	1.8	0.7	0.7	0.7	0.8
Th	7.4	5.8	6.8	15.3	4.8	5	4	4.2
U	3.6	2	2.8	6.8	1.8	2.2	1.5	1.6
V	8	<8	<8	<8	20	15	42	16
Zr	321.3	336.1	339.5	178.8	400.1	327.6	266.2	388.4
Y	42.9	38	43	94.7	36.2	34.9	30.1	37.8
La	28.9	30.6	33.2	30.7	26.4	24.3	23	25
Ce	69	70.1	74.6	75.6	58.4	53.8	50.4	57.9
Pr	7.67	8.1	8.73	8.39	7.16	6.4	5.89	7.31
Nd	31.4	32.2	33.4	31.7	29	26.2	23	30.1
Sm	6.52	6.51	7.45	7.92	6.4	5.75	4.85	7.05
Eu	1.12	1.32	1.23	0.27	1.54	1.31	1.16	1.61
Gd	6.77	6.62	7.44	8.88	6.34	5.87	5.12	6.66
Tb	1.16	1.1	1.24	1.89	1.06	1.03	0.89	1.13
Dy	7.66	6.86	7.92	13.88	6.33	6.61	5.31	6.7
Ho	1.64	1.45	1.61	3.14	1.22	1.32	1.08	1.4
Er	4.92	4.08	4.71	10.4	3.82	4.13	3.26	4.15
Tm	0.76	0.65	0.74	1.71	0.59	0.6	0.47	0.62
Yb	5.45	4.53	5.01	11.77	4.04	4.35	3.2	4.45
Lu	0.84	0.66	0.79	1.82	0.63	0.66	0.51	0.7

#### 4.1 Major elements geochemistry

The major element concentrations are plotted against SiO<sub>2</sub> on the Harker diagrams (Fig.4) to reveal the relationships among these variables with the progress of magmatic processes. From these

plots, it is clear that  $\text{Al}_2\text{O}_3$ ,  $\text{Fe}_2\text{O}_3$ ,  $\text{TiO}_2$ ,  $\text{CaO}$ ,  $\text{P}_2\text{O}_5$ , and  $\text{MnO}$  negatively correlate with  $\text{SiO}_2$  while  $\text{K}_2\text{O}$  shows positive correlation with  $\text{SiO}_2$ .  $\text{Na}_2\text{O}$  displays poor-defined trends with  $\text{SiO}_2$  consistent with what was reported by Bateman and Dodge (1970) that the  $\text{Na}_2\text{O}$  concentrations don't vary systematically with differentiation. The negative correlation between  $\text{Al}_2\text{O}_3$ ,  $\text{Fe}_2\text{O}_3$ ,  $\text{TiO}_2$ ,  $\text{CaO}$ , and  $\text{MnO}$  and  $\text{SiO}_2$  can be attributed to the fractional crystallization processes. Negative correlation between  $\text{CaO}$  and  $\text{SiO}_2$  can be attributed to the fractional crystallization of plagioclase. The decrease in  $\text{P}_2\text{O}_5$ ,  $\text{MgO}$  and  $\text{FeO}$  during magmatic evolution indicates separation of apatite and mafic mineral (such as biotite) during crystallization.  $\text{TiO}_2$  decrease with increasing silica content may be due to the formation of Ti-magnetite and/or ilmenite.

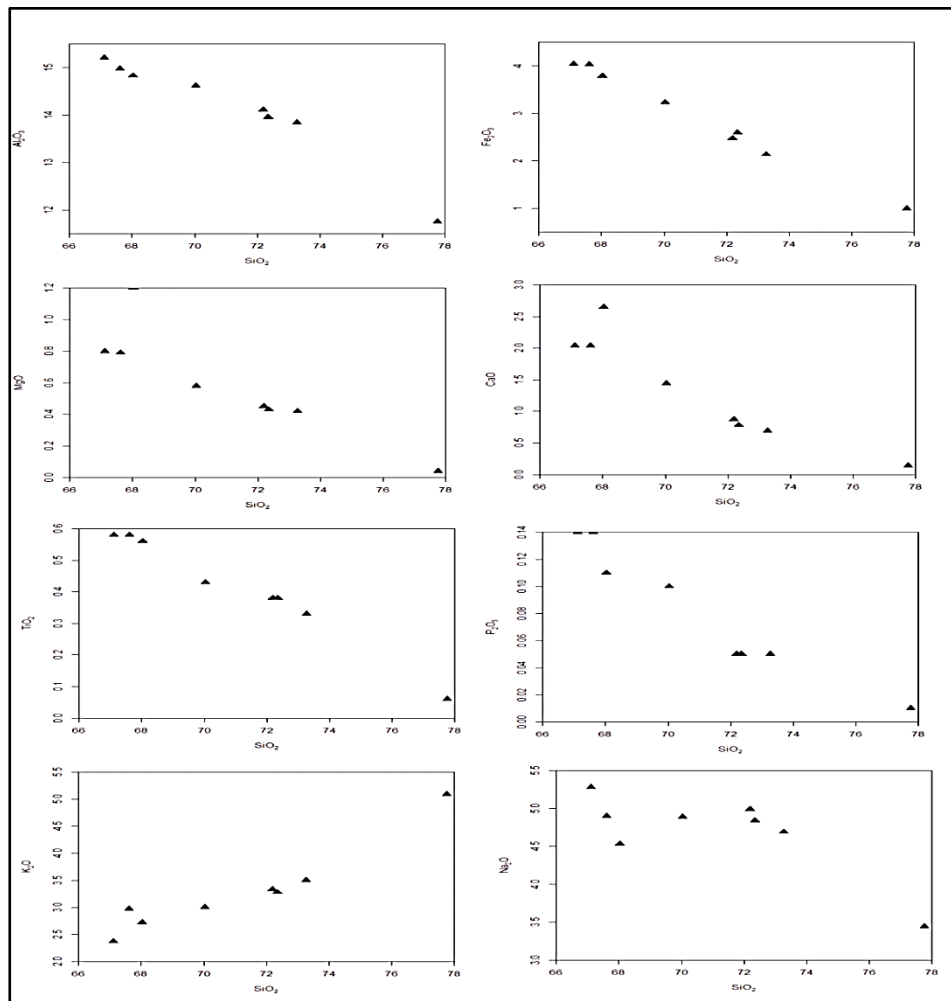


Fig.4: variation diagrams (major oxides vs.  $\text{SiO}_2$ )

#### 4.2 Petrochemical classification

Streckeisen (1976) used the normative minerals albite, orthoclase, and anorthite to classify the granitic rocks (Fig.5a). According to this classification, the studied granitic rocks fall mostly within the fields of monzogranite and syenogranite except for one sample that falls within the alkali feldspar granite field. By plotting the studied granitic rocks on the classification diagram suggested by Cox et al (1979) (Fig.5b), they fall within the field of granite. The majority of data points were plotted within the field of granite on the classification diagram suggested by De Le Roche et al. (1980) (Fig.5c).



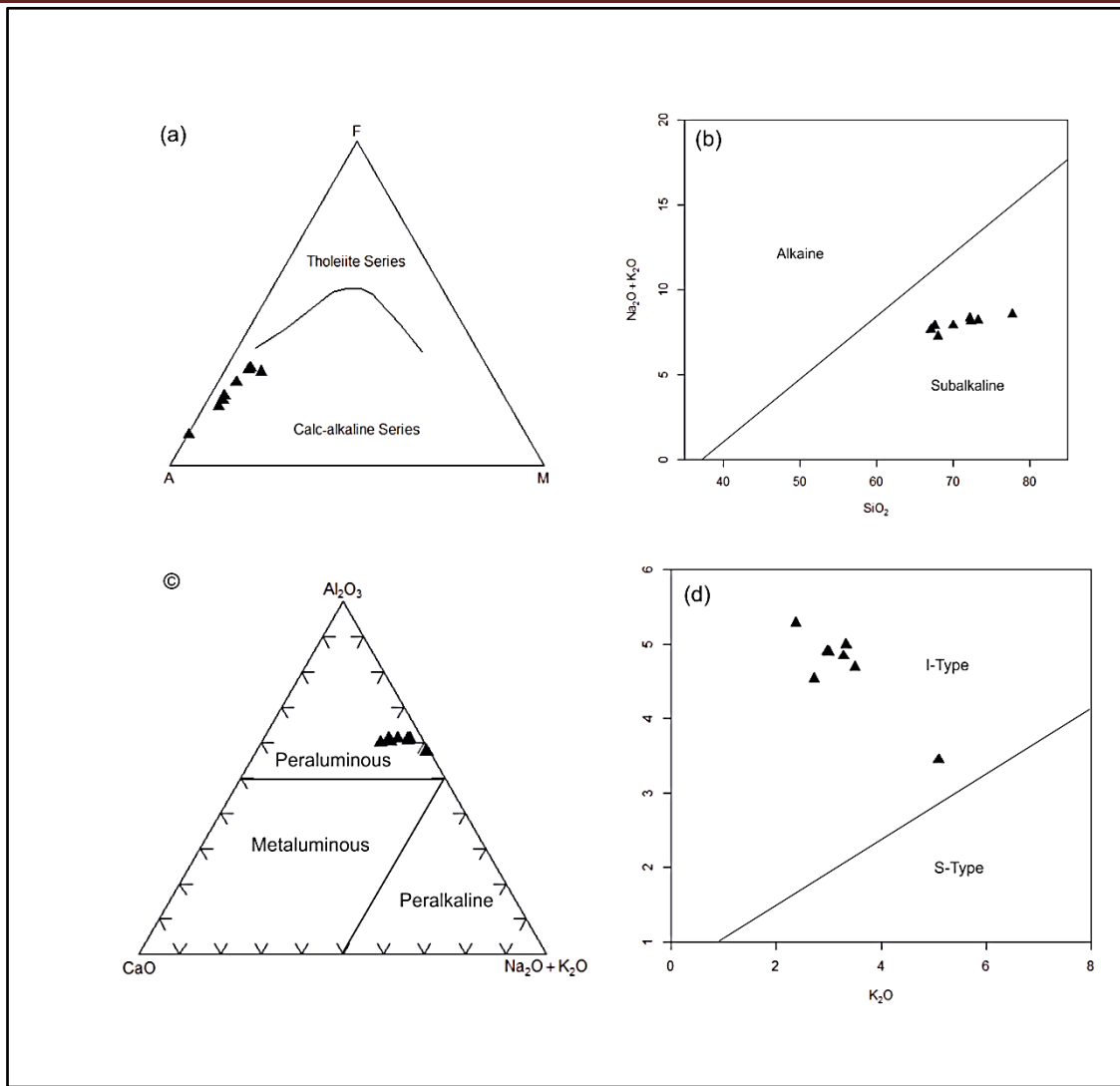


Fig.6: Magma type discrimination diagrams.(a) AFM ternary diagram of Irvine and Baragar (1971), (b)  $\text{SiO}_2$  vs.  $(\text{Na}_2\text{O} + \text{K}_2\text{O})$  (Irvine and Baragar, 1971), (c)  $\text{CaO}-\text{Al}_2\text{O}_3-(\text{Na}_2\text{O} + \text{K}_2\text{O})$  (Shand, 1951), (d)  $\text{K}_2\text{O}$  vs.  $\text{Na}_2\text{O}$  (White and Chappell, 1974).

#### 4.4 Tectonic setting

The two groups of the incompatible elements 1) large ion lithophile elements (LILE) and 2) high field strength elements (HFSE) can be used as indicators of the magmatic processes and tectonic settings for the formation of granitic rocks. The first group includes elements with large ionic radii e.g., K, Rb, Sr, Ba and Cs, while the second contains elements with higher valencies including Zr, Th, U, Ta, REE etc. various discriminant diagrams based on LILE and HFSE are used for the determination of tectonic settings of granitic rocks (Pearce et al., 1984). The Rb versus  $\text{Ta} + \text{Yb}$  (Fig.7a) (Pearce, 1982), Rb versus  $\text{SiO}_2$  (Fig.7b) (Pearce et al., 1984), and Nb versus  $\text{SiO}_2$  (Fig.7c) (Pearce and Gale, 1979) discriminant diagrams are employed here to investigate a probable tectonic setting of the Atalla I-type younger granites. On the basis of these diagrams, the studied samples fall within the volcanic arc. The abundance of Niobium element can be used to discriminate between the tectonic setting of magmas responsible for the formation of volcanic-arc granites and within-plate granites (Pearce and Gale, 1979). The Nb abundance in volcanic-arc granites is markedly lower (<14 ppm) than that in within-plate granites (with Nb content exceeding 100 ppm) across the entire range of  $\text{SiO}_2$ . On this basis, all the studied Atalla granitoids show volcanic arc magmatic setting. On the tectonic discrimination  $(\text{Na}_2\text{O} + \text{K}_2\text{O})-\text{FeO}-\text{MgO}$  ternary diagram (Fig.7d) introduced by Petro et al

(1979), the studied granitoid rocks make an angle with the AF side which suggested that these rocks were formed in compressional regime rather than extensional regimes.

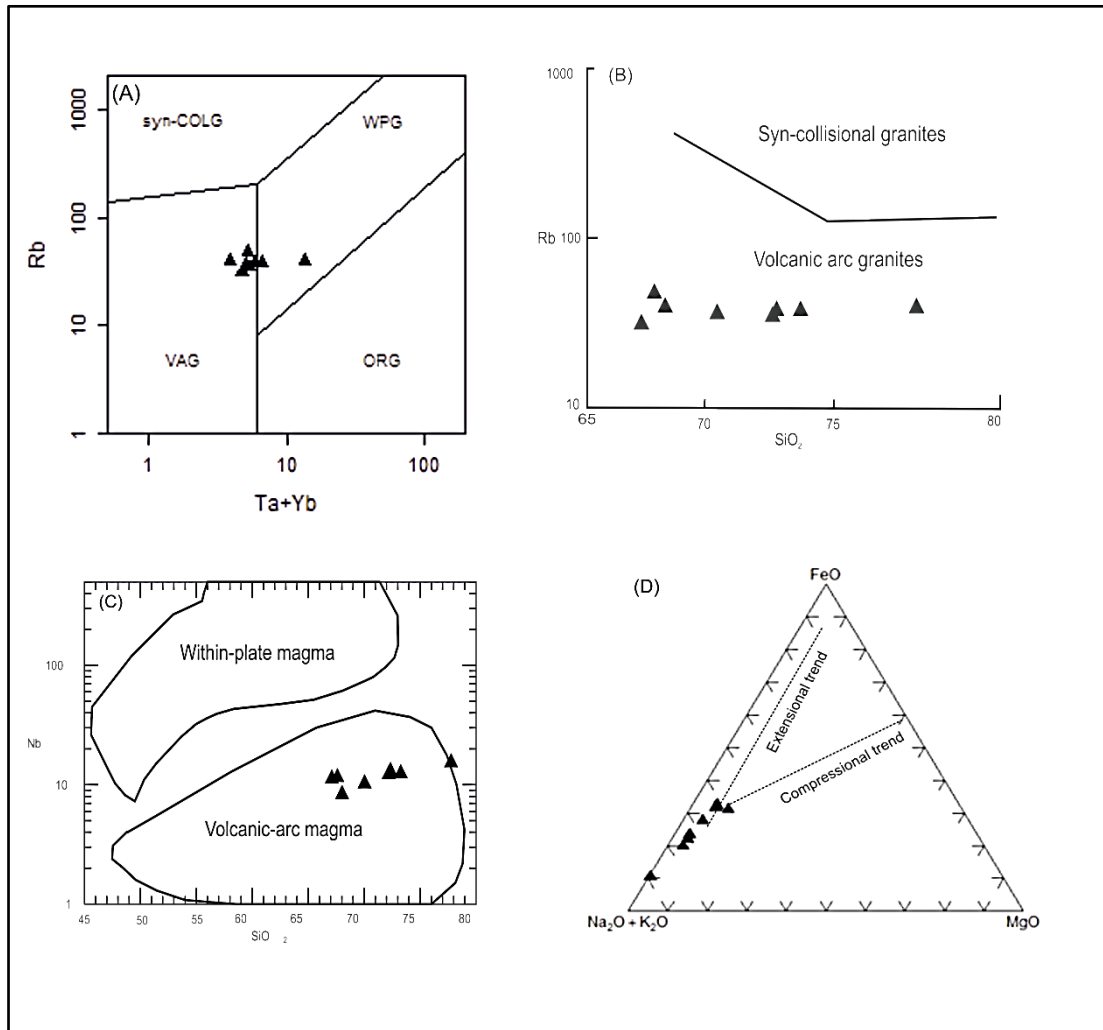


Fig.7: Tectonic setting discrimination diagrams: (a) Rb vs. Ta+Yb (Pearce et al., 1982), (b) Rb vs. SiO<sub>2</sub> (Pearce et al., 1984), (c) Nb vs. SiO<sub>2</sub> (Pearce and Gale, 1979), (d) Na<sub>2</sub>O+K<sub>2</sub>O-FeO-MgO ternary diagram (Petro et al., 1979).

#### 4.5 Petrogenesis

The presence of mafic rocks associated with these granites indicates that they were derived from mantle rather than crustal material. On the K-Rb binary diagram (Fig.8a), all the studied granites plot around the mantle line (K/Rb=1000) suggested by Shaw (1968) and away from the crustal line (K/Rb=250) given by Taylor (1965). This reflects their low K concentrations that suggest their derivation from upper mantle source rather than upper crustal materials. Moreover, on the constructed the K-Ba binary diagram (Fig. 8b) (Mason, 1966) All the plots are located below the average crustal line (K/Ba=65), showing relatively low K enrichment and K/Ba ratio less than 65, except one sample plots above the crustal line. The studied granite samples plotted on this diagram supports their derivation from a mantle material. The Ba/Rb ratios are more sensitive than K/Rb ratio in tracing the differentiation in K-feldspars (Taylor and Heier 1960). On the Ba-Rb binary diagram of Mason (1966)(Fig. 8c), the studied granite samples are plotted above the crustal line (Ba/Rb=4.4) favoring derivation of these granites from partial melting of mantle materials.

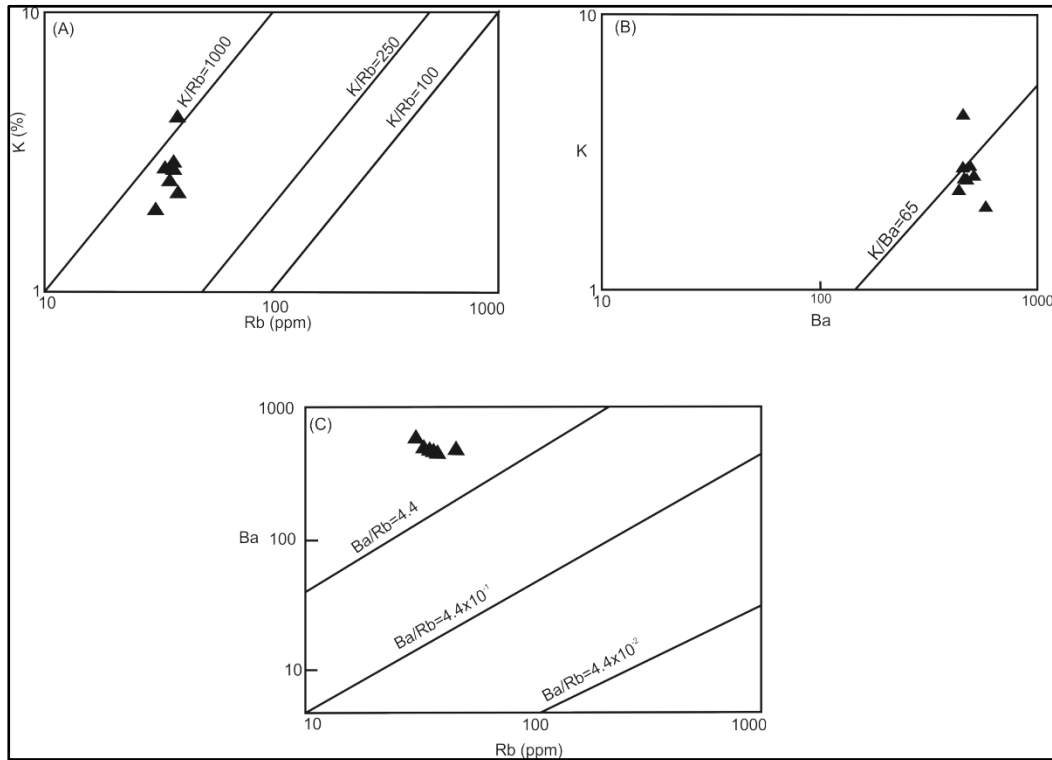


Fig.8: (a) K vs. Rb diagram (Shaw 1968) shows the average crustal K/Rb ratio of Taylor (1965), (b) K-Ba binary diagram. The average crustal K/Ba ratio after Mason (1966), (c) the Ba-Rb binary diagram (Mason 1966).

## References

- Abdel-Rahman, A. M. and Martin, R. F., 1990. The Mount Gharib A-type granite, Nubian Shield: petrogenesis and role of metasomatism at the source. *Contributions to Mineralogy and Petrology*, 104, 173-183.
- Akaad M. K. and Noweir A. M., 1980. Geology and lithostratigraphy of the Arabian Desert orogenic belt of Egypt between Lat. 25° 35' and 26° 30' N. *Institute of Applied Geology of Jeddah, Bulletin*, 4, 127-134.
- Akaad, M. K., Noweir, A. M. & Kotb, H., 1979. Geology and petrochemistry of the granite association of the Arabian Desert Orogenic Belt between latitudes 25 35' and 26 30' N. *Delta J. Sci.*, 3, 107 - 151.
- Bateman, p.c., and Dodge, F.C.W., 1970. Variations of major chemical constituents across the central sierra Nevada, batholith: *Geological society of America bulletin*, v.18, p. 409-420.9.
- Bentor YK (1985) The crustal evolution of the Arabo-Nubian Massif with special reference to the Sinai Peninsula. *Precambrian Res* 28:1-74.
- Cox, K. G, Bell, J. D., Pankhurst, R. J., 1979. The interpretation of igneous rocks. George Allen & Unwin, London, United Kingdom, 450p.
- De La Roche, H., Leterrier, J., Grand-Claude, P., Marchal, M., 1980. A classification of volcanic and plutonic rocks using R1-R2 diagram and major element analyses. Its relationship with current nomenclature. *Chemical Geology*, 29, 183- 210.
- El-Sayed, M. M., 1998. Tectonic setting and petrogenesis of the Kadabora pluton: a late Proterozoic anorogenic A- type younger granitoid in the Egyptian Shield. *Chemie der Erde*, 58, 38-63.
- El Bouseily, A. M., Ghoneim, M. F., Arslan, A. L & Harraz, H. Z., 1985. Contribution to the petrography and geochemistry of G. Atalla granite, Central Eastern Desert, Egypt. Abstract, 23rd Annual Meeting of the Geological Society of Egypt, Cairo.
- El Gaby, S., List, F. K. and Tehrani, R., 1988. Geology, evolution and metallogenesis of the Pan-African belt in Egypt. In: S. El Gaby and R.O. Greiling (Eds.). *The Pan-African belt of Northeast Africa and adjacent areas. Earth Evolution Sciences*, Vieweg, Wiesbaden.
- El Kassas, I. A. & Bakhit, F. S., 1989. Geology of Wadi Atalla – El Missikat area, Eastern Desert, Egypt. *Qatar Univ. Sci. Bull.*, 9, 227 -244.
- El Kassas, I. A., 1974. Radioactivity and geology of Wadi Atalla area, Eastern Desert of Egypt. Ph. D. Thesis, Fac. Sci., Ain Shams Univ., Cairo, 502p.
- Gass .I.G (1982) Upper Proterozoic (Pan-African) calc alkaline magmatism in northeastern Africa and Arabia. In: Thorpe RS (ed), *Andesites*. Willey, pp 591-609.
- Hassan, M. A., and Hashad, A. H., 1990. Precambrian of Egypt. In Said, R. (Ed.), *The geology of Egypt*. Balkma, Rotterdam, 201-245.
- Hassanen, M. A., 1997. Post-collision, A-type granites of Homrit Waggat complex, Egypt: petrological and geochemical constraints on its origin. *Precambrian Research*, 82, 211-236.
- Hussein, A. A., Ali, M. M. and El-Ramly, M. F., 1982. A proposed new classification of the granites of Egypt. *Journal of Volcanology and Geothermal Research*, 14, 187-198.
- Irvine, T., Baragar, W., 1971. A guide to the classification of the common volcanic rocks. *Canadian journal of Earth Science*, 8, 523-548.
- Kröner A (1993) The Pan-African Belt of Northeastern and Eastern Africa, Madagascar, Southern India, Sri Lanka and East Antarctica terrane amalgamation during formation of the Gondwana super continent. In: Thorweihe U, Schandelmeier H (eds) *Geoscientific research in Northeast Africa*. Balkema, Rotterdam, pp 3-9.
- Kröner A, Eyal M, Eyal Y (1990) Early Pan-African evolution of the basement around Elat, Israel, and the Sinai Peninsula revealed by single-zircon evaporation dating, and implications for crustal accretion rates. *Geology* 18:545-548.
- Mason B (1966) *Principals of geochemistry*, 3rd edn. Jhon Wileys Sons, New York, p 610.
- Noweir AM, Sewiftm BM, Abu El Ela AM (1990) Geology, petrography, geochemistry and petrogenesis of the Egyptian younger granites. *Qatar Univ Sci Bull* 10:363-393.

- Pearce, J. A, Harris NBW, Tindle AG (1984) Trace element discrimination diagrams for the tectonic interpretation of granitic rocks. *J Petrol* 25:956–983.
- Pearce, J. A., 1982. Trace element characteristics of lavas from destructive plate boundaries: in Thorpe, R.S. (Editor): *Andesites*, John Wiley and Sons, Chichester, p. 525-548.
- Pearce, J. A., and Gale, G. H., 1979. Identification of ore deposition environments from trace elements geochemistry of associated igneous host rocks. *Journal of the Geological Society*, London, Spec. Pub. 134, 14-24.
- Pearce, J. A., Harris, N. B. and Tindle, A. G., 1984. Trace element discrimination diagrams for the tectonic interpretation of granite rocks. *Journal of Petrology*, 25, 956-983.
- Petro, W. L., Vogel, T. A. and Wilband, J. T., 1979. Major elements chemistry of plutonic rocks suites from compressional and extensional plate boundaries. *Chemical Geology*, 26, 217-235.
- Shand S.J., 1951. *The study of rocks*. London, Thomas Murby and Co.236p.
- Shaw DM (1968) A review of K-Rb fractionation trends by covariance analyses. *GeochimCosmochimActa* 32:573–601.
- Stern, R. J (1993) Tectonic evolution of the late Proterozoic EastAfrican Orogen constraints from crustal evolution in the ArabianNubian Shield and the Mozambique Belt. In: Thorweihe U, Schandelmeier H (eds) *Geoscientific research in NortheastAfrica*. Balkema, Rotterdam, pp 73–74.
- Stern, R. J, Hedge CE (1985) Geochronologic and isotopic constraints on late Precambrian crustal evolution in the Eastern Desert of Egypt. *Am J Sci* 258:97–127.
- Stern, R. J, Sellers G, Gorrfried D (1988) Bimodal dike swarms in the northeastern Desert of Egypt Significance for the origin of Late Precambrian "A-type" granites in Northern Afro Arabia. In: El Gaby S, Greiling R (eds), *The Pan-African Belt of NE Africa and Adjacent Areas*. Wisbaden, pp. 147-179.
- Stern, R. J, Sellers G, Gorrfried D (1988) Bimodal dike swarms in the northeastern Desert of Egypt Significance for the origin of Late Precambrian "A-type" granites in Northern Afro-Arabia. In: El Gaby S, Greiling R (eds), *The Pan-African Belt of NE Africa and Adjacent Areas*. Wisbaden, pp 147-179.
- Streckeisen A, Le Maitre RW (1979) A chemical approximation to the modal QAPF classification of the igneous rocks. *N Jahrb Mineral Abh* 136:169–206.
- Taylor SR (1965) The application of trace element data problems in petrology. In: Ahrens LH, Press F, Runcor SR, Urey HC (eds). *Physical and chemical of the earth*, pp 133-213.